Silver-Palladium Electrodeposition on Unsupported Vulcan XC-72R for Oxygen Reduction Reaction in Alkaline Media

Melissa Vega-Cartagena,[1,*] Elena M. Flores-Vélez,[2] Guillermo S. Colón-Quintana,[1] Daniel A. Blasini Pérez,[3] Marco A. De Jesús,[2] Carlos R. Cabrera[1,*]

[1]Department of Chemistry, Molecular Sciences Research Center, University of Puerto Rico, Río Piedras Campus, San Juan, PR 00925-2537

[2]Department of Chemistry, University of Puerto Rico, Mayagüez Campus, Mayagüez, PR 00680

[3]Department of Biology, University of Puerto Rico, Río Piedras Campus, San Juan, PR 00925-2537

* Corresponding authors: melissa.vega@upr.edu; carlos.cabrera2@upr.edu

ABSTRACT

Carbon-supported Ag-Pd bimetallic nanocatalysts were successfully synthesized via the rotating disk slurry electrode (RoDSE) technique in a nominal precursor solution as a cost-effective means to improve oxygen reduction reaction (ORR) performance in fuel cell (FC) applications. Silver and palladium have both individually shown good catalytic activity. The work presented here compares three different electrodeposition methods using RoDSE, a robust electrodeposition method that allows the synthesis of highly dispersed Ag/Pd nanoparticles on Vulcan XC-72R, minimizing the catalyst preparation time. The electrochemical methods consist of (1) alternated, (2) sequential, and (3) simultaneous Ag and Pd electrodeposition on unsupported Vulcan XC-72R. Different characterization techniques such as TEM, XRD, ICP, and Raman spectroscopy were used to confirm the presence of Ag and Pd on the carbon substrate. The Ag/Pd face centered cubic crystal facets were determined by XRD with an approximate particle diameter of 23 nm for each electrochemical method. Performance of the catalysts was assessed for the ORR using cyclic voltammetry and rotating disk electrode techniques. Herein, we demonstrate that among the three methods of bimetallic Ag/Pd electrodeposition, an alternated approach yielded the best performance, measured using onset potential (E_{onset}), peak current density, and electron transfer in an alkaline media, in O_{2}- saturated 0.1 M KOH.

KEYWORDS: *Oxygen reduction reaction, silver, palladium, unsupported electrodeposition, bimetallic catalyst, Vulcan, RoDSE*

BACKGROUND

Most of the energy produced in recent times comes from fossil fuels that are limited both in use and availability. More importantly, their use has a profound and detrimental effect to the environment, in particular, greenhouse gas emissions and climate change[1]. Given the need to reduce the human dependence on fossil fuels, researchers have focused their attention on cleaner energy alternatives.[2, 3] Ever-growing energy demand has directed modern society towards the use of alternative energy sources such as solar, wind, geothermal, and hydroelectric, amongst others, to produce electricity.[4] A growing market of alternative fuel generation involves the use of fuel cells[3], which directly generate electricity through simple yet environmentally friendly hydrogen oxidation reaction (HOR) and ORR processes.[2, 4] The oxygen reduction occurs in the cathode, while fuel is oxidized into water in the anode.[2] This cell configuration has the potential to alleviate energy supply problems while offering significant advantages such as high efficiency, zero environmental pollution, low cost, and an unlimited source of necessary reagents.[5]

ORR is a critical reaction for fuel cell operation: it is an irreversible reaction which involves several reduction steps, which in turn produces oxygen-containing species such as O, OH^-, $O_2^{-\bullet}$, HO_2^- and H_2O_2, depending on the electrolyte and the solution.[3,6,7] When ORR is carried out in an alkaline solution, electron transfer can occur by two key pathways: **(1)** the 4-e^- reduction pathway converts O_2 directly to H_2O and **(2)** the 2-e^- reduction pathway converts O_2 to H_2O, producing hydrogen peroxide (H_2O_2) as an intermediate compound.[3,8,9] Although H_2O_2 is a natural disinfectant with some medical uses, peroxide formation in FCs decreases efficiency, lowers cell voltage, facilitates membrane degradation, and contributes to the corrosion process of some metals.[8,9] As a result, there is a need to develop innovative FCs with reaction pathways that minimize peroxide production while favoring water production. Despite the prospective production of H_2O_2 as natural disinfectant for medical purposes, better cathode materials are needed for energy generation.[3]

Several mechanisms have been proposed to describe the ORR process, but these are not very well understood.[3,6,7] One of the mechanisms that has recently gained scientific acceptance is the process by which oxygen is reduced to the superoxide anion, followed by further reduction to the H_2O_2 anion, and finally to the hydroxide anion as shown in the following reaction steps:[3,8-10]

$$O_2 + e^- \rightarrow O_2^{\bullet-} \quad (1)$$

$$O_2 + H_2O + 2e^- \rightarrow HO_2^- + OH^- \ (2e^-) \qquad E^o = -0.076 \text{ V vs SHE} \quad (2)$$

$$HO_2^- + H_2O + 2e^- \rightarrow 3OH^- \ (2e^-) \qquad E^o = 0.878 \text{ V vs SHE} \quad (3)$$

From an electrochemical standpoint, the 4-e^- reduction pathway is preferred because it is the ideal energy storage and conversion process for devices such as FCs and metal-air batteries on alkaline electrochemical media. However, the drawback is that the strong molecular oxygen double bond must first be broken.[7]

Recent studies have proposed electrocatalysts that can carry out more efficient reduction of oxygen to water. These include noble metals (e.g. Pd, Pt, and Au)[3], alloys (e.g. Ag–Co, Ag-Cu, Pt-Co)[4,11,12], iron-based catalysts (e.g. $FePSe_3$)[13], carbon materials (e.g. carbon black, graphene)[3], and quinone (e.g. the anthraquinone process)[11], among others.[6,14] These electrocatalysts can be prepared in diverse ways depending on the purpose and materials needed. Several FC studies have reported the modification of the electrode surface with noble metal nanoparticles (NPs) such as: Pt, Au, and Pd.[7] Among the tested metals, Pt has proven to be the optimal catalyst for ORR application since it favors the 4-e^- pathway, which equates to a complete reduction of oxygen to water.[2,7] Unfortunately, due to its high cost and low abundance, efforts must be made to find a viable substitute.[2,7] Ag has demonstrated attributes that make it a viable candidate for the replacement of Pt, mainly due to it being far less expensive (70:1).[12,15,16] Ag NPs have proven to be reasonably abundant, durable, low toxic, and highly active in the ORR reaction in alkaline media.[1,2,6,17] In addition, because Ag is maintained in its metallic state during ORR, it is an excellent catalyst for the reduction of H_2O_2 and for hydrogen oxidation. The equilibrium potential between Ag and Ag_2O is 1.17 V vs. RHE, which is below the equilibrium potential between O_2 and H_2O, which is 1.23 V.[4]

The process of Ag NP fabrication requires careful control of the chemical composition and conditions since the nanoparticles are prone to high levels of aggregation. This process is governed by strong Van Der Waals forces, because of extremely high surface energy in Ag clusters, which can promote the loss of chemical sensitivity and electrochemical activity.[9, 18] To minimize performance loss, Ag NPs are doped on either organic or inorganic substrates that serve as a protective media while improving the available surface area of the active sites by circumventing particle aggregation and enhancing its catalytic activity and stability.[9] The substrate material for the deposition of a metal should supply as many nucleation sites as possible, to prevent NP agglomeration while minimizing particle size.[19] Carbon based substrates are most commonly used for these applications, due to their superior properties: excellent conductivity, high surface area, fabrication simplicity, low cost, and minimal electrical noise.[17] However, studies have shown that the sole use of Ag on a carbon support possesses inferior electrocatalytic activity towards ORR due to its weak oxygen binding energy compared to metals such as Pt.[20] Therefore, to enhance the performance of Ag, a bimetallic aggregate of Ag and Pd was developed. This work was accomplished by optimizing for the amount of added Pd to maximize catalytic performance vs. cost.

Different methodologies have been employed for the development of bimetallic nanoaggregates as catalysts. RoDSE is a technique developed by Santiago et al.[21-23] in which

isolated atoms, clusters or metallic NPs are electrodeposited on colloidal conductive carbon supports. This is done under hydrodynamic electrodeposition conditions. This technique consists of dissolving metal precursor salts in a carbon support slurry in which a constant reducing potential is applied to a glassy carbon rotating disk electrode (RDE). A constant rotating frequency speed is used to achieve the metal electrodeposition on the carbon support instead of the RDE glassy carbon electrode. With this technique, the electrodeposition occurs because the metal NPs are electrochemically reduced by two main pathways: (1) when the metal ions under study and the surface of the glassy carbon working electrode come into contact and (2) when the carbon support is charged enough, by the glassy carbon working electrode, to reduce the metal ion to a metallic state when it comes in contact with surface of the RDE mentioned before.[21] This technology is very useful, because it has several advantages: monitoring the size and distribution of the NP, avoiding their agglomeration, and controlling and varying the loading of metal particles that are added to the slurry to produce a hybrid material in powder form,[21] The RoDSE technique has been studied for the electrodeposition of metal NPs using different kinds of support such as Vulcan XC-72R[24], carbon nano-onions[25], single wall carbon nanotubes[25], graphene oxide[26], and zeolites.[27] To our knowledge, the RoDSE technique has not been used to electrodeposit the combination of Ag and another precious metal on a carbon support as described in this work.

Herein, an efficient electrocatalyst was synthesized consisting of Ag/Pd nanoparticles with a nominal precursor solution mass ratio of 4:1 (Ag:Pd) using Vulcan XC-72R as carbon support. The mass ratio was calculated using the weight of the metal added from the metal salt precursor solution, rather than the volume of the solution. The 4:1 Ag:Pd ratio was based on a previous study of Ag/Pd bimetallic catalysts by Slanac *et al* (2012) in which the ORR mass activity for Ag_4Pd was 598 mA/mg_{metal}, which struck a balance between catalytic activity and cost. When compared to a 9:1 ratio for Ag_9Pd (340 mA/mg_{metal}), the mass activity for 4:1 is superior while still using comparable amounts of palladium.[10] Additionally, Ag_4Pd's surface has more efficient heteroatomic sites and Pd activity per weight due to the catalyst's single Pd atoms being surrounded by Ag atoms, resulting in a mass activity 3.2 times that of a theoretical linear combination of Ag and Pd, and 4.7 times that of pure Pd.[10] With respect to the carbon support, it has a specific surface area of ca. 250 m^2g^{-1}, because is the most commonly used in the preparation of commercial catalysts due its good properties between electrical conductivity, high surface area and it is less expensive.[17] Herein, bimetallic catalysts are successfully synthesized, using the RoDSE technique with three different electrodeposition methods: (1) alternated, (2) sequential, and (3) simultaneous. These catalysts were then tested for the ORR in alkaline media, in O_2-saturated 0.1 M KOH solution.

EXPERIMENTAL SECTION

Electrocatalysts Preparation

All of the catalyst samples were synthesized using the RoDSE technique with minor changes to the conditions previously reported by Santiago et al.[22] As mentioned previously, the RoDSE technique consists of dissolving a metal salt precursor in a slurry carbon solution while a reduction potential is applied to a rotating glassy carbon working electrode. This promotes the nanoparticle reduction on the conducting substrate, as shown in Figure 1. The RoDSE technique uses a typical three-electrode cell assembly. In one compartment, a reference electrode is placed, consisting of a reversible hydrogen electrode (RHE). At the center, the working electrode is a glassy carbon rotating disk electrode (RDE, glassy Carbon (GC), Pine Research Instruments), with a geometric area of 0.20 cm^2, which rotates at 2000 rpm in the slurry solution. The last compartment contains a Pt wire auxiliary electrode. Each of the three compartments contains an aqueous sulfuric acid solution (0.1 M). All of the catalyst electrodepositions were done by applying a constant reductive potential of 0.4V vs. RHE. Twelve aliquots of a solution containing 5.0 mM of $AgNO_3$ (Sigma Aldrich) and $C_4H_6O_4Pd$ (Sigma Aldrich) metal salt precursor in 0.1M H_2SO_4 were added in 20-minute intervals. Again, the mass ratio of 4:1(Ag:Pd) was used and compared to commercial E-TEK 20 wt.% Pt on Vulcan.

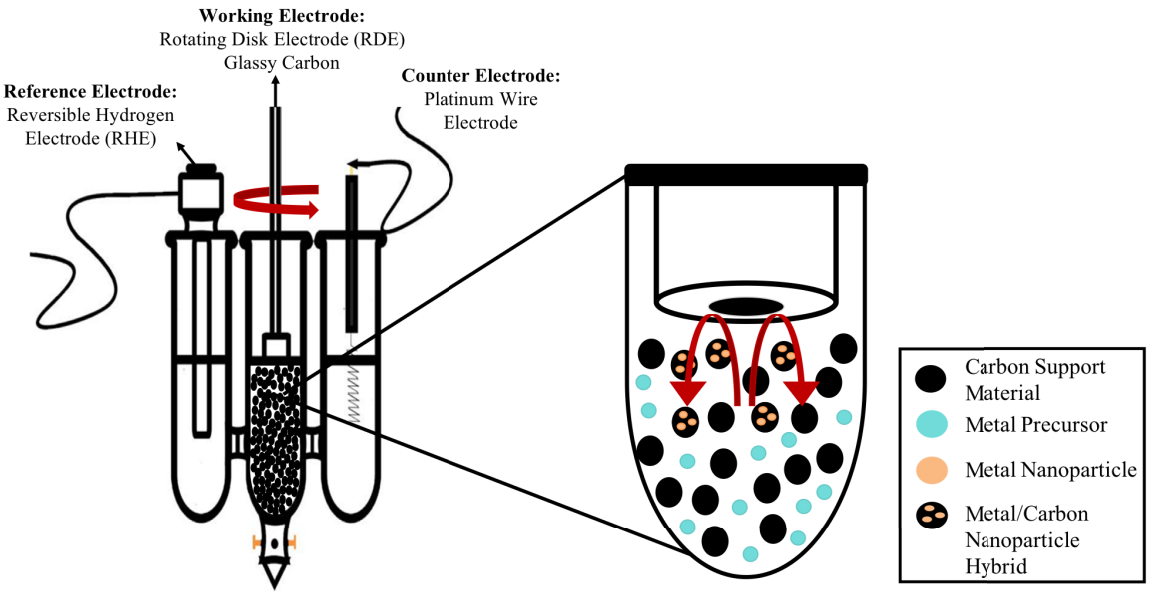

Figure 1. General setup of the RoDSE technique. Electrochemical arrangement of a three-electrode cell using RHE as the reference electrode, glassy carbon as the rotating working electrode, and a platinum coiled wire as the counter electrode in 0.1M H_2SO_4. At the center of the cell, precursor solution aliquots are added to a carbon slurry.

Preparation of Ag/V and Pd/V catalyst

A suspension was prepared in a beaker containing 50 mg of Vulcan XC–72R nanoflakes (Cabot Corporation) and 20 mL of 0.1 M H_2SO_4 (Optima, Fisher). Then, 50 mg of Vulcan in 1.0 M H_2SO_4 was placed under ultrasound for 4 hours prior to the RoDSE experiment. This increases the nucleation sites on the surface of the carbon particles and creates a well disperse slurry.[24] For Ag, a reductive potential of 0.4V vs RHE was applied after every addition of 1 mL of a solution of 5mM $AgNO_3$ metal salt precursor with a period of 20 minutes for a total of 4 hours of electrodeposition time at 2000 rpm. Afterwards, the slurry was filtered and rinsed with nanopure water (18.2 MΩ-cm EDM Milli-Q Direct 16). The catalyst was then dried in a 65°C oven for 24 hours and ground to a fine powder for use in the relevant characterization. Then, a clean glassy carbon electrode (GCE) was used for the catalyst ink modification. The GCE was carefully and sequentially polished prior the experiment with an alumina oxide ranging from 1.0 to 0.05 μm (Buehler Micropolish). The catalyst ink consisted on 1 mg of catalyst powder mixed with 140 μL of ethanol (99.5% Sigma Aldrich) and 10 μL of Nafion solution (5% solution in alcohol, Sigma Aldrich). The GCE was introduced to 2 μL of the ink and then air dried at room temperature for 30 minutes to obtain the modified GCE. A similar procedure was applied for preparation of Pd/Vulcan XC-72R using $C_4H_6O_4Pd$ and for the Ag/Pd/Vulcan XC-72R bimetallic samples.

Preparation of Ag/Pd/V catalyst

Alternated Electrodeposition

An alternated Ag and Pd electrodeposition on Vulcan XC-72R was performed in twelve electrodeposition steps of 20 minutes each. Ag/Pd/Vulcan XC-72R was prepared using an electrodeposition of Ag and then Pd onto Vulcan XC-72R. First, 2 mL of $AgNO_3$ metal salt precursor was added to the slurry solution. Then, after 20 min, an aliquot containing 0.4 mL of Pd from a 5 mM $C_4H_6O_4Pd$ solution was added. This chronoamperometry process was cycled for a total of 12 times. These electrodepositions were done under an applied constant potential of 0.4 V vs. RHE. This potential is kept constant for all of the electrodepositions described hereafter.

Sequential Electrodeposition

A sequential electrodeposition of Ag and Pd on Vulcan XC-72R was done in twelve steps in a similar fashion as the alternated electrodeposition method. However, the order in which the aliquots were transferred was changed. For this sample, six 2 mL aliquots of Ag were added every 20 min from the 5mM of $AgNO_3$ solution to the slurry solution, and then six 0.4 mL

aliquots from the Pd 5 mM $C_4H_6O_4Pd$ solution were added every 20 min to complete the twelve electrodepositions.

Simultaneous Electrodeposition

A simultaneous electrodeposition of Ag and Pd on Vulcan XC-72R was done in twelve electrodepositions as in the previous process. The difference here consists of the simultaneous addition of both aliquots ($AgNO_3$ and $C_4H_6O_4Pd$). For this sample, twelve 1 mL aliquots were added to the slurry every 20 min from the 5mM of $AgNO_3$ solution. At the same time for each step, twelve 0.2 mL aliquots of 5 mM $C_4H_6O_4Pd$ solution were added.

Characterization Measurements

All electrochemical measurements were done using a three-electrode SP-50 potentiostat/galvanostat (Biologic Instruments). The RDE system was used to perform the synthesis of all the samples in the RoDSE technique and for the hydrodynamic voltammetry in the ORR. The current densities present in this work were normalized using the geometrical surface area of the electrodes. Wide-angle x-ray diffraction (WAXD) was performed on carbon supported catalyst powder on a quartz slide with a Rigaku Ultima IV X-Ray diffractometer using Cu Kα radiation (1.54 Å). Sample diffraction patterns were collected at a scan rate of 3°/min at 0.02° steps from 10° to 90°. High-resolution transmission electron microscopy (HRTEM) and scanning transmission electron microscope (STEM) was conducted using a FEI Tecnai F-20 microscope operated at 200 keV and an Oxford X-Max detector. The carbon supported catalysts were deposited on a 200-mesh copper grid coated with lacey carbon. Inductively Coupled Plasma–Optical Emission Spectrometry (ICP–OES) was performed to measure Ag and Pd metal catalyst loading using an Optima 8000 Perkin Elmer ICP–OES. Herein, 10 mg of each bimetallic catalyst was dissolved prior to the analysis with 10 mL of aqua-regia solution and simmered until an ink paste remained. The solutions were passed through a Whatman glass microfiber filter (GF / F grade) and diluted with 2% HNO_3 solution in a volumetric flask. Quantification of all samples was performed using an external calibration curve. Raman analyses were done using Xplora confocal Raman microscope (Horiba Scientific, Co.) with back scattering configuration. Spectra were acquired with 600 grooves/mm grating and an average of 90 scans with a 30 second irradiation at 638 nm and 2.35 mW laser power.

RESULTS AND DISCUSSION

Surface Analysis

High resolution transmission electron microscopy (HRTEM) analysis was done to investigate the surface morphology of the catalysts synthesized using the RoDSE technique. HRTEM shows a contrast in density, which confirms the presence and formation of both metals. While Ag metals appear as dark spots, Pd metals are seen as brighter spots. Figure 2 shows images for Ag/Pd catalysts supported on Vulcan in alternated, sequential, and simultaneous methods. Different sizes were observed in which quasi-spherical shape and nano-size scales were predominant. The bimetallic catalyst had average particle sizes of 21.1, 28.1, and 30.9 nm for the alternated, sequential, and simultaneous methods, respectively. In all of the bimetallic samples, highly aggregated NPs were observed, which correspond to Ag NPs on the Vulcan substrate. Figures 2a and 2d of the Ag/Pd in alternated method show a high tendency for the agglomeration of Ag and Pd particles deposited. They show a strong tendency for the agglomeration of Ag particles deposited on the carbon support with moderately small Ag and Pd nanoparticles in comparison to the other methods. Ag/Pd in the sequential method (Figures 2b and 2e) appear to be more uniform in comparison with the alternated method. For Ag/Pd, in the simultaneous method (Figures 2c and 2f), moderated Ag and Pd NPs are homogeneously dispersed on the carbon substrate. In addition, elemental mapping using scanning transmission electron microscope (STEM) was performed for Ag and Pd in the alternated (g), sequential (h), and simultaneous (i) methods, respectively. These images confirm the presence of both metals in the bimetallic catalyst and confirms that of the methods under study, the sequential method shows the most uniform distribution. Figure 3 shows the particle size histogram and demonstrates the tendency of particle agglomeration as the method was varied. The sequential method showed the most uniform distribution of particle agglomeration.

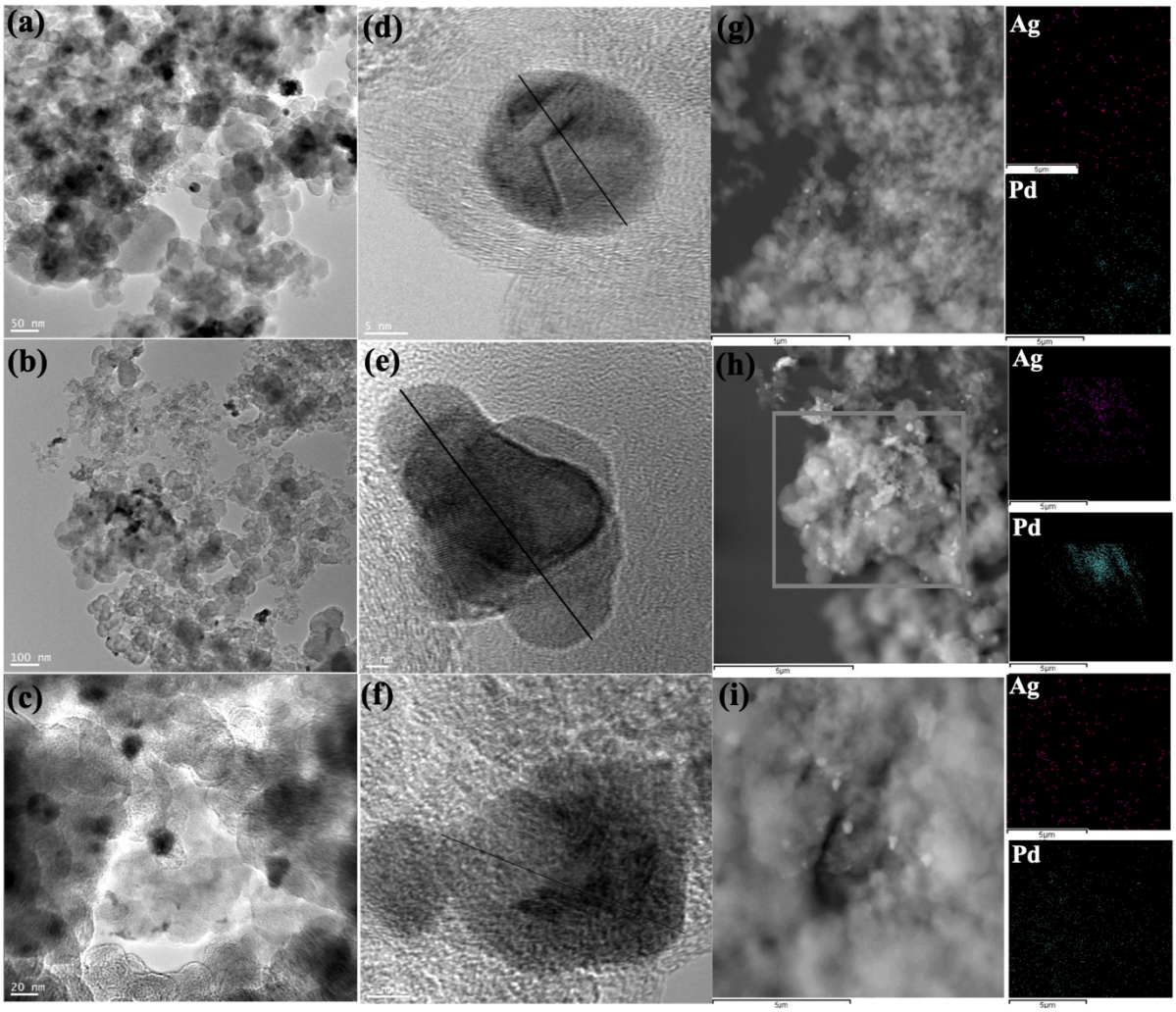

Figure 2. HRTEM images of Ag/Pd/Vulcan catalyst prepared by RoDSE alternated (a and d), sequential (b and e), and simultaneous (c and f) methods; STEM for elemental mapping of Ag and Pd in (g) alternated, (h) sequential, and (i) simultaneous methods.

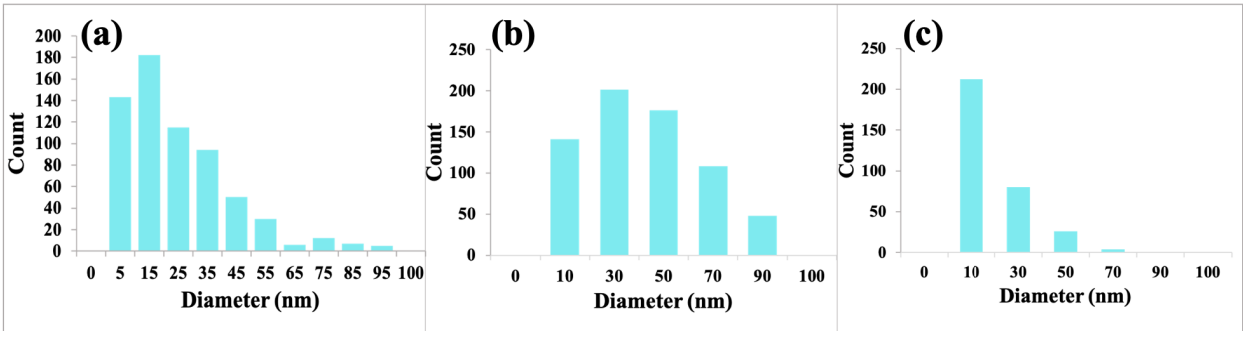

Figure 3. Particle size histogram, in nanometers, from HRTEM images for Ag/Pd/Vulcan catalysts prepared by RoDSE (a) alternated, (b) sequential, and (c) simultaneous methods.

Physicochemical characterization

X-ray diffraction (XRD) analysis was performed to compare the crystal structure of the synthesized Ag, Pd, and Ag/Pd catalysts on Vulcan XC-72R for the alternated, sequential, and simultaneous methods (Figure 4A)**.** The XRD pattern of all the samples showed a face centered cubic (FCC) structure with common peaks located at 38.5°, 44.9°, 65.0°, 77.8°, and 79.9°, which come from the diffraction indices of (111), (200), (220), (311), and (222) expected for both Ag and Pd. With the incorporation of Pd, the bimetallic sample XRD data exhibit minor shifts to a lower angle with broader and more symmetrical peaks (Figure 4B). These minor shifts show that the incorporation of Pd atoms into the Ag lattice and vice versa allow the formation of a bimetallic catalyst.[2] The average crystalline size of the bimetallic catalysts was calculated from Ag (111) using Scherrer's formula.[16] The average sizes are in a range of 21 to 29 nm, which are consistent with TEM results (Table 1). XRD data indicate dominance of the Ag (111) peak in the bimetallic catalyst samples.

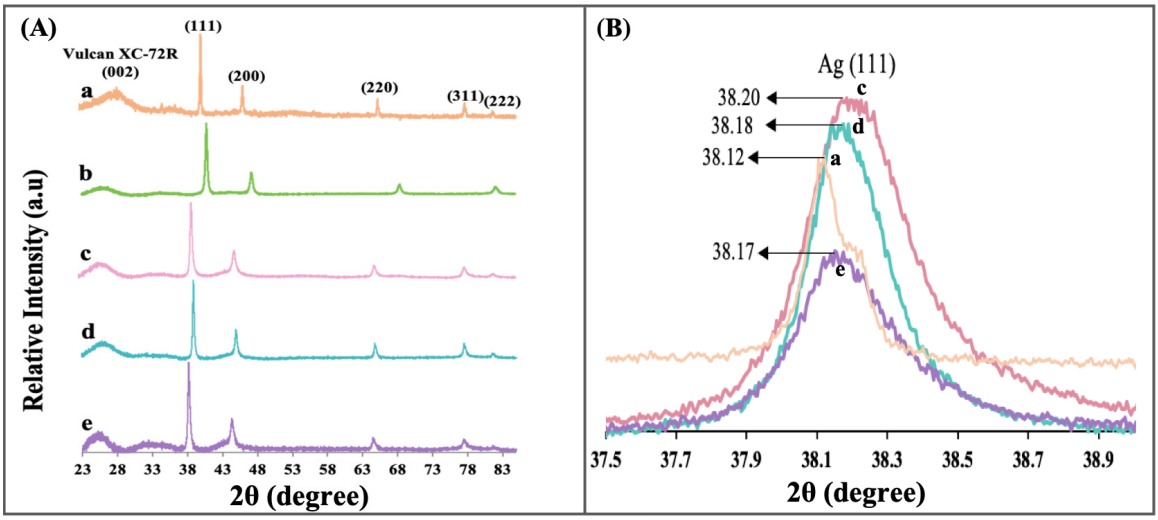

Figure 4. X-ray diffraction (A) and expanded XRD spectra for the Ag (111) peak (B) for: (a) Ag, (b) Pd and Ag/Pd catalysts unsupported on Vulcan XC-72R prepared by RoDSE (c) alternated, (d) sequential and (e) simultaneous methods. The broad peak from 23° to 30° is linked to the Vulcan XC-72R carbon support.

Table 1. Summary of catalyst characterization morphology, by TEM and XRD analysis, for Ag/Pd catalysts in the different RoDSE electrodeposition methods (alternated, sequential, and simultaneous).

Catalyst	Size (nm) TEM	Size (nm) XRD
Ag/Pd/Vulcan Alternated	21.1	21.3
Ag/Pd/Vulcan Sequential	28.1	27.2
Ag/Pd/Vulcan Simultaneous	30.9	28.8

Raman spectroscopy has been used as a tool to assess structural changes of sp^2 carbons and its charge transfer effects of allotropic forms of carbon and carbon clusters such as graphite, graphene and graphene oxide materials.[2, 28-38] Several studies have demonstrated that Vulcan XC-72R has similar physicochemical characteristics to graphite, in particular, describing it as an amorphous mesoporous graphitic material.[2, 28] Vibrational analysis show two bands at 1594 cm^{-1} and 1348 cm^{-1} corresponding to the characteristic G and D vibrations of carbon.[29] The G vibration is characteristic of in-plane stretching vibration of sp^2- hybridized carbon-carbon bonds, whereas D vibration occurs as a result of the structural disorder of the carbon atoms.[30] Previous studies have shown that G band shift to lower frequencies upon addition of Ag to graphene oxide.[29, 30] As shown in Figure 5A, the G band on 1603 cm^{-1} corresponds to untreated Vulcan, while Ag/Vulcan and Ag/Pd/Vulcan shift to 1591 cm^{-1}, which is close to the value of pure graphite. Such a band shift to a lower wavenumber is indicative of a charge transfer effect between Vulcan and Ag/Pd and is reflected as a decreased bond order of the sp^2 carbons. Thus, this confirms the reduction conditions employed for the preparation of the catalyst and the incorporation of Ag and Ag/Pd to Vulcan material. The intensity ratios of D and G bands (I_D/I_G) are another factor used to assess structural changes and metallic interactions on carbon substrates such as Vulcan. The observed Vulcan and Ag/Vulcan I_D/I_G ratios were 1.1(±0.3) and 1.0(±0.4), respectively (Figure 5B). For the Ag/Pd/Vulcan alternated, Ag/Pd/Vulcan sequential, and Ag/Pd/Vulcan simultaneous catalysts, the observed ratios were of 1.1(±0.2), 1.0(±0.2), and 1.0(±0.1), respectively. Intensity changes in the carbon G band provide information on changes in carbon particle distribution within the Vulcan clusters, because of chemical reduction processes. As expected, there was a slight decrease in the intensity of the G band, which indicates a more effective reduction on the Ag/Vulcan, Ag/Pd/Vulcan sequential and Ag/Pd/Vulcan simultaneous samples. Although the results show a slight improvement in carbon particle distribution for these nanocatalysts, the changes are within the uncertainty range of the I_D/I_G, indicating that there are no substantial differences in the Vulcan chemistry upon the synthesis of the nanocatalyst. However, the small reduction of I_D/I_G ratio for Ag/Pd/Vulcan sequential can be attributed to lower reduction efficiency of the process, indicating higher sp^2 C conformation. Moreover, Ag/Pd/Vulcan Sequential had a shifted D band to higher wavenumbers

(1351 cm^{-1}) indicating conformational changes on the aromatic ring. These changes are indicative of a more uniform distribution of the bimetallic catalyst within Ag/Pd/Vulcan sequential method followed by simultaneous and alternated method, respectively.

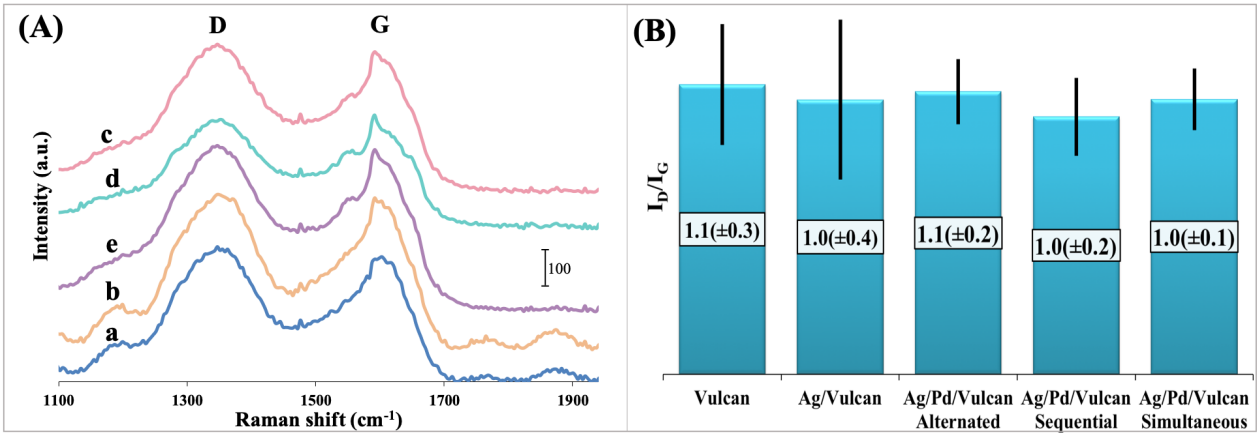

Figure 5. (A) Raman spectra and (B) Intensity ratios of D and G Raman bands for (a) Vulcan XC-72R, (b) Ag/Vulcan and bimetallic Ag/Pd supported in Vulcan XC-72R prepared by RoDSE (c) alternated, (d) sequential, and (e) simultaneous methods.

ICP–OES was performed to determine the percentage of the total Ag and Pd loading in each bimetallic catalyst sample. Herein, Ag/Pd supported on Vulcan synthesized using the simultaneous method contains the most Ag and Pd by mass, followed by the alternated and sequential method, respectively (Table 2). Although a small amount of Ag was electrodeposited in the sample, it is noteworthy that the values in the percentages do not vary notably with respect to one method or the other. This leads us to the conclusion that the RoDSE technique provides consistent results.

RoDSE Electrodeposition

Figure S1 shows the electrodeposition chronoamperometry of Ag (Figure S1a), Pd (Figure S1b), Ag/Pd in alternated (Figure S1c), sequential (Figure S1d), and simultaneous (Figure S1e) RoDSE methods on Vulcan XC-72R. This figure shows the cathodic currents obtained for each added aliquot of the precursor solution in deposition of Ag in the Ag sample (Figure S1a), Pd in the Pd sample (Figure S1b), and both Ag and Pd in the three methods under study on Vulcan XC-72R using the RoDSE technique. As mentioned above, the differences in the electrodeposition addition vary only in the order in which the twelve aliquots were added. For the bimetallic catalysts and for the standards, it may be observed that the average deposition current increased in relation of the applied electrodeposition method. For an electrodeposition potential of 0.4V vs. RHE, the average maximum deposition cathodic current was −350 mA, −380 mA, and −390 mA for alternated, sequential, and simultaneous, respectively.

Tables S1 and S2 shows the chronoamperometry data results of the electrodeposition time in terms of the percentages of Ag and Pd, respectively, that are electrodeposited onto Vulcan XC-72R using the RoDSE technique. Tables S1 and S2 shows the chronoamperometry data results in combination with the chronoamperometry deposition profile (Figure S2 and S3) in terms of the percentages of Ag and Pd, respectively, that are electrodeposited onto Vulcan XC-72R using the RoDSE technique. Using the ICP values and assuming that the percentage of recovery is the same in each step, it was determined that the maximum percent of both metals electrodeposited on the Vulcan slurry is 0.12($\pm$0.003) %, 0.12($\pm$0.009) % and 0.14($\pm$0.008) % of Ag in the alternated, sequential, and simultaneous method respectively, as determined from charge integrated from each electrodeposition plot and metal percent (Table 2). Moreover, we observe 1.21($\pm$0.020) %, 2.27($\pm$0.070) %, and 2.5($\pm$0.3) % for Pd on Vulcan, in the alternated, sequential, and simultaneous methods, respectively (Table 2). In the chronoamperometric data, the maximum percentages of both metals electrodeposited on the Vulcan slurry are 3.80 %, 3.60%, and 5.0% of Ag and 1.70%, 2.50%, and 3.70% for Pd on Vulcan in the alternated, sequential, and simultaneous methods, respectively.

The final catalyst metal loading as determined by ICP (w/w %), specifically for Ag, are a little below those obtained in the chronoamperometry. These concentrations of metals are the initial concentrations prior to chronoamperometric reduction. These were the initial concentrations when preparing the catalytic batch. After synthesis, the concentration and the recovery percent were determined by ICP under the same conditions, whereby the results were determined with the corresponding error bars. In order to quantitatively know how much of the metal was remaining at the end of the electrodeposition, the percentages of metal transfer onto the catalyst were determined: for Ag, 3.2%, 3.3%, and 2.8% and for Pd, 71.2%, 90.8%, and 67% for the alternated, sequential, and simultaneous methods respectively. These results show very little Ag recovery. In the case of ICP-OES, we need to consider that the use of aqua-regia for digestion in the preparation of the samples. Because aqua-regia contains HCl, it is possible that during the preparation of ICP-OES samples, AgCl precipitate was formed.[39] However, it is also possible that the Ag NPs did not dissolve properly in HNO_3, HCl at certain ratios (3:1 is usually ideal to improve solubility) may have resulted in the accumulation of non-solubilized Ag sticking to the container surface.[39] The use of sulphuric acid may have also resulted in the reduction of Ag NPs via the formation of silver sulphides.[39] Any presence of water could have resulted into the formation of undesired silver hydroxides or oxides on the surface of the tubing, rather than mixed into the solution (more unlikely with a more acidic solution). This suggest that the concentrations obtained in the chronoamperometric were only theoretical.

Table 2. Summary of bimetallic catalyst characterization data of the loading by ICP and Chronoamperometric measurements for Ag, Pd and Ag/Pd catalysts in the different RoDSE electrodeposition methods (alternated, sequential, and simultaneous).

Catalyst	Initial metal concentration for chronoamperometric synthesis (w/w%)				Final Catalyst Metal Loading as determined by ICP (w/w %)				% Metal Transfer onto Catalyst			
	%Ag	95% CL	%Pd	95% CL	%Ag	95% CL	%Pd	95% CL	Ag	95% CL	Pd	95% CL
Ag/Pd/Vulcan Alternated	3.80	1.99	1.70	0.75	0.12	±(0.003)	1.21	±(0.02)	3.2	1.5	71.2	29.8
Ag/Pd/Vulcan Sequential	3.60	1.74	2.50	1.24	0.12	±(0.009)	2.27	±(0.07)	3.3	1.7	90.8	37.3
Ag/Pd/Vulcan Simultaneous	5.00	2.48	3.70	1.74	0.14	±(0.008)	2.5	±(0.3)	2.8	0.1	67	24.8
Ag/Vulcan	5.40	2.88	-	-	0.20	±(0.02)	-	-	3.6	1.9	-	-
Pd/Vulcan	-	-	4.80	2.34	-	-	3.1	±(0.007)	-	-	92.1	40.0

Electrochemical Characterization

Electrocatalytic Activity

All of the electrochemically prepared catalysts using the RoDSE method were characterized by cyclic voltammetry in Ar-purged 0.1M KOH solution. Figure 6 shows the cyclic voltammograms displaying the characteristic redox peaks for Ag (Figure 6a), Pd (Figure 6b), Ag/Pd in alternated (Figure 6c), sequential (Figure 6d), and simultaneous (Figure 6e) RoDSE methods, all supported in Vulcan XC-72R.

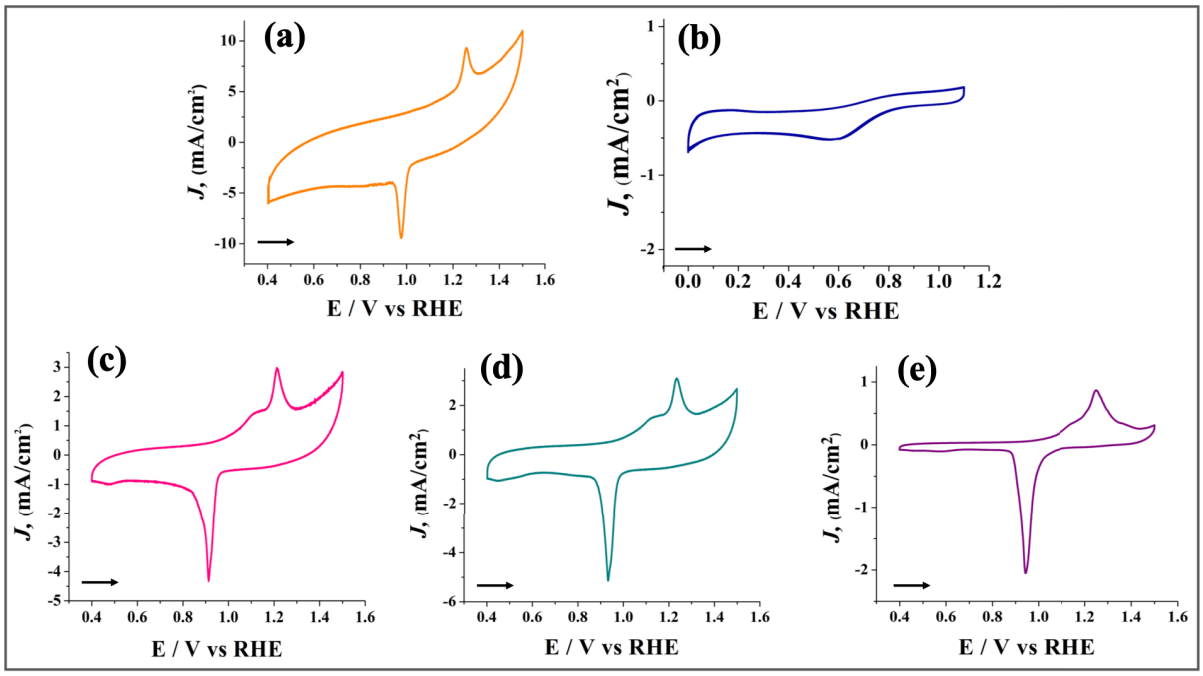

Figure 6. Cyclic voltammograms of a Glassy Carbon Electrode modified with: (a) Ag/Vulcan and Ag/Pd/Vulcan prepared by (b) Pd/Vulcan, (c) alternated, (d) sequential, and (e) simultaneous RoDSE methods in Ar-saturated 0.1M KOH solution at a scan rate of 20 mV s^{-1}. The arrows indicate the potential sweep direction, from left to right to positive values.

Herein, for Ag/Vulcan XC-72R (Figure 6a), in a potential window of 1.20 to 1.35 V vs. RHE, has one oxidation peak that is attribute to the formation of the Ag_2O layer and one reduction peak in a potential window of 0.90 to 10.50V vs. RHE that correspond to the oxide reduction Ag_2O to Ag^0. These results are in agreement with CV's previously reported in the literature.[16] For Pd, the main difference observed is that the Pd (II) oxide layer reduction peak is around 0.50 V vs. RHE. From this observation, the higher potential limits are moved more positively with an increase in cathodic current and a shift to lower potential values. Here, a Pd cathodic peak around 0.60 V vs. RHE was observed, corresponding to the deposition of Pd onto the GCE. Therefore, it is important to note that electrodeposition of a solution in the suspension may differ than the electrodeposition just in the solution, because of the presence of carbon flakes that may cause depolarization of the Pd deposition. Moreover, these bimetallic CV's show mostly Ag features; however, with the incorporation of Pd, the observed peaks in a potential window between 0.90 V to 1.30 V vs. RHE in the anodic region are due to the Ag oxygen adsorption and desorption reactions.[40] In addition, in the cathodic region, a small additional peak around 0.40 to 0.60 V vs. RHE corresponds to Pd oxide reduction. An increase in the magnitude in the Ag oxidation peak and a minor shift to negative potential in the reduction peak represents

a stronger oxygen adsorption interaction with Ag in the presence of Pd.[16, 27] The curves for the bimetallic catalysts show the presence of both Ag and Pd reduction peaks in the surface catalyst.

Electrocatalytic Oxygen Reduction Reaction

The electrocatalytic activity of the catalyst synthesized using the RoDSE technique was characterized by studying the oxygen reduction reaction (ORR). Hydrodynamic voltammetry on each catalyst using the RDE technique was done and the potential at which the number of electrons transferred is 0.65V vs. RHE for all catalysts.

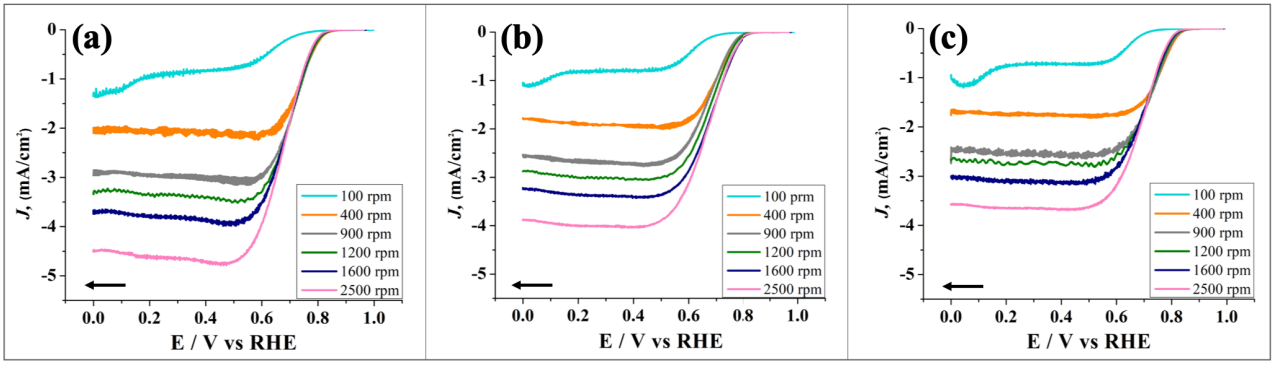

Figure 7. The rotating-disk electrode voltammograms for electrochemically reduced Ag/Pd/Vulcan in (a) alternated, (b) sequential, and (c) simultaneous methods by RoDSE technique in O_2-saturated 0.1 M KOH solution at a scan rate of 20 mV/s^{-1} at different rotation speeds, 100, 400, 900, 1200, 1600 and 2500 rpm. The arrows indicate the potential sweep direction, from right to left to negatives values.

Figure 7 shows the ORR polarization curve of Ag/Pd in the alternated (Figure 7a), sequential (Figure 7b), and simultaneous (Figure 7c) electrodeposition methods at 0.1M KOH. Steady-state polarization of the bimetallic catalysts was performed at rotation speeds of 100, 400, 900, 1200, 1600, and 2500 rpm and were recorded at a scan rate of 20 mV/s^{-1}. Fig.7 shows a direct proportional relation between the current density and rotation speed: as the rotation speed increases, the current density increases linearly.

Table 3. Data obtained for the ORR derived from hydrodynamic polarization curve of catalysts prepared by RoDSE.

Catalyst	Onset Potential (V)	Half wave Potential (V vs RHE)	No. of electrons
Ag/Vulcan	0.654	0.559	2.10
Pd/Vulcan	0.831	0.711	3.67
Commercial 20% Pt/Vulcan	0.901	0.780	4.01
Ag/Pd/Vulcan Alternated	0.811	0.694	3.94
Ag/Pd/Vulcan Sequential	0.803	0.682	3.27
Ag/Pd/Vulcan Simultaneous	0.818	0.705	3.12

The ORR onset potential (E_{onset}) in the three bimetallic catalysts remain similar (Table 3). In addition, the half-wave potential ($E_{1/2}$) for the different catalysts was determined to have values in the range from 0.559 V to 0.780 V. In the bimetallic catalysts, we observe significantly reduced diffusion-limiting currents. Moreover, in terms of onset potential, the Ag/Pd synthesized using the simultaneous method has an overpotential of approximately 83 mV less than Pt/C in 0.1M KOH at 1600 rpm. The $E_{½}$ of the three bimetallic catalysts also remain very similar (Table 3). ORR polarization curves demonstrate that the $E_{1/2}$ of Ag/Pd in the alternated, sequential, and simultaneous methods had a positive shift of 86, 98, and 75 mV, respectively, relative to commercial Pt/Vulcan. This can be attributed to the strong interactions of the catalysts with the electrodes. This demonstrates that the bimetallic catalysts may achieve higher activity than the metals by itself. Herein, the Ag/Pd synthetized by RoDSE technique demonstrated an excellent performance in ORR efficiency in terms of the E_{onset}, $E_{1/2}$, e^- transfer and the current density that it produced under the circumstance that they were can be well synthetized.

To compare the catalytic activity of different bimetallic catalysts (Ag/Vulcan, Pd/Vulcan, and Pt/Vulcan) for the ORR, and to determine the mechanism by which the ORR is carried out, oxygen polarization at 1600 revolutions per minute was performed to increase the O_2 diffusion on the catalyst surface. A scan rate of 20 mVs^{-1} was used to obtain the number of electrons (*n*) transferred for each O_2 molecule in the ORR activity (Figure 8). The electrochemical and hydrodynamics properties of RDE are correlated with the Koutecky−Levich (K−L) equation, which determines the number of electrons transferred, using the slope of the plotted points. This gives us insight into how many electrons (*n)* are flowing during the reaction using the following equation: [16, 10]

$$\frac{1}{j} = \frac{1}{j_k} + \frac{1}{j_d} = \frac{1}{nFkC_0} + \frac{1}{0.62nFC_0(D_0)^{\frac{2}{3}}v^{\frac{-1}{6}}\omega^{\frac{1}{2}}} \quad (4)$$

In equation (4), j_k is the kinetic-limiting current density, j_d is the limiting current density, n is the number of transferred electrons in the reaction, F is the Faraday constant (96485.34 C mol^{-1}), k is the electron transfer rate constant, C_o is the bulk concentration of O_2 in the electrolyte involved (1.2 mM L^{-1})[2], D_o is the diffusion coefficient of O_2 (2 x 10^{-5} cm^2s^{-1}) [2,41], ν is kinematic viscosity of the electrolyte (1 x 10^{-2} cm^2s^{-1})[2], and ω is angular velocity in rad/s (2πN, N is the linear rotation speed).[2,14,41] Koutecky-Levich plots are shown in supplemental Figures S4 to S6 and the corresponding n-E dependencies are given in Figure S7. Most of the catalysts present linear relationships between the limiting current density and the rotation rate.

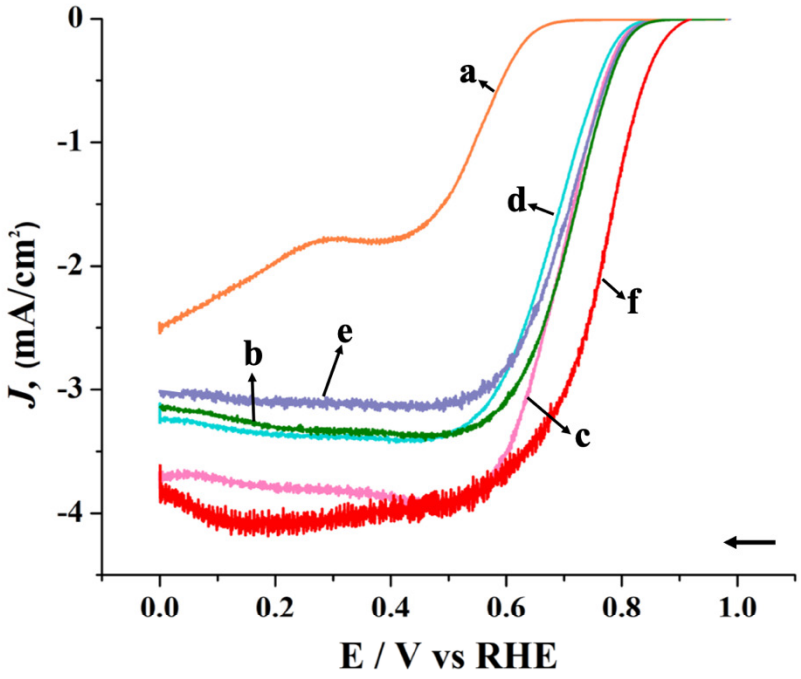

Figure 8. Linear sweep voltammograms from RDE measurement in O_2- saturated 0.1M KOH solution at scan rate of 20 mV s^{-1} at 1600 rpm for catalysts: (a) Ag/Vulcan, (b) Pd/Vulcan, (c) Ag/Pd/Vulcan alternated, (d) Ag/Pd/Vulcan sequential, (e) Ag/Pd/Vulcan simultaneous, and (f) 20%Pt/Carbon Vulcan. The arrows indicate the potential sweep direction, from right to left to negatives values.

From the slopes presented in Figure 8, the n values were calculated to be 3.94, 3.27, and 3.12 for Ag/Pd in the alternated, sequential, and simultaneous electrodeposition methods, respectively (Table 3). It can be seen that both Pd/Vulcan and commercial Pt/Vulcan show a

greater limiting diffusion current in comparison with Ag/Vulcan and the bimetallic catalyst. This is probably due to the low Ag content on the electrode where the ORR could be catalyzed by the Vulcan XC-72 carbon via the 4-e^- pathway. Figure 8 shows the oxygen polarization curve in which Ag/Pd demonstrates superior catalytic activity for ORR in terms of E_{onset}, limited current density, and facilitated electron transfer. This indicates a very high efficiency for the direct oxygen reduction in alkaline media in comparison with the other electrodeposition methods. The electron transfer number for Pt/Vulcan is 4, which, when compared to the synthetized bimetallic catalysts, is indicative of a promising catalyst.

To further investigate ORR pathways, the potential dependencies of the calculated number of transferred electrons, *n*, are shown in Figure S7. Interestingly, the *n* value of Ag/Pd/Vulcan prepared by the alternated method is close to 4: the n-value decreases to 3.60 at a potential of 0.30 V and then gradually increases to 3.94, suggesting a four electron pathway. In addition, we observe that there exists a small influence of the ORR on different electrocatalysts in alkaline medium, leading to values between 2.10 and 3.94 for the number of electrons exchanged. The difference in activity between the bimetallic catalysts can be mainly attributed to two reasons: the arrangement between the Ag and Pd in the carbon due to different preparation methods and the difference in particle size. Ag/Pd/Vulcan prepared using the alternated method has a lower particle size than the sequential and simultaneous method, respectively.

CONCLUSIONS

In this work, carbon-supported Ag/Pd NPs bimetallic electrocatalysts were synthesized via the RoDSE technique. This technique was tested in three different methods of electrodeposition of Ag and Pd with the purpose of forming bimetallic particles onto Vulcan XC-72R. XRD analysis demonstrated the presence of all of the expected peaks of Ag and Pd, with a minor shift to a lower angle which suggests the formation of an alloy. In the bimetallic CVs, a negative potential shift in the Ag oxide peak was observed when compared to Ag/Vulcan. This indicates an activity increase in the ORR. In Raman spectroscopy, Ag/Pd on Vulcan using the sequential method had a shifted D band to higher frequencies and demonstrated a more uniform distribution than the bimetallic catalyst. From the ORR results for all catalysts, when adding Pd to Ag, better ORR activity was achieved and demonstrated that the bimetallic proceeds primarily through a 4-electron pathway in comparison to Ag/Vulcan and Pd/Vulcan. However, of the catalysts synthesized using different methods, Ag/Pd using the alternated method demonstrated superior ORR catalytic performance. However, results from TEM and ICP demonstrate that we need to optimize the applied electrodeposition potential for both metals, especially Ag, in order to obtain a higher metal loading. These studies demonstrated that RoDSE technique can be used for the electrodepositions for more than one metal and, therefore, is a promising bimetallic catalyst preparation method.

ACKNOWLEDGMENTS

This work was supported by the National Science Foundation NSF-PREM: Center for Interfacial Electrochemistry of Energy Materials (CiE^2M) grant number DMR-1827622 and NSF-CREST Center for Innovation, Research and Education in Environmental Nanotechnology ($CIRE^2N$) grant number HRD-1736093. This work made use of the Cornell Center for Materials Research Shared Facilities, which are supported through the NSF MRSEC grant number DMR-1719875.

Supporting Information Available: The following file is available free of charge. Supporting Information RoDSE Ag_Pd_ORR. The supporting information material presents the chronoamperometric plots and tabulated data of the RoDSE electrodeposition of Ag, Pd, and Ag/Pd.

References

1. Neumann, C. C. M.; Laborda, E.; Tschulik, K.; Ward, K. R.; Compton, R. G., Performance of silver nanoparticles in the catalysis of the oxygen reduction reaction in neutral media: Efficiency limitation due to hydrogen peroxide escape. *Nano Res.* **2013,** *6*, 511-524.
2. Joo, Y.; Ahmed, M. S.; Han, H. S.; Jeon, S., Preparation of electrochemically reduced graphene oxide-based silver-cobalt alloy nanocatalysts for efficient oxygen reduction reaction. *Int. J. Hydrog. Energy* **2017,** *42*, 21751-21761.
3. Ge, X.; Sumboja, A.; Wuu, D.; An, T.; Li, B.; Goh, F. W. T.; Hor, T. S. A.; Zong, Y.; Liu, Z., Oxygen Reduction in Alkaline Media: From Mechanisms to Recent Advances of Catalysts. *ACS Catal.* **2015,** *5*, 4643-4667.
4. Holewinski, A.; Idrobo, J.-C.; Linic, S., High-performance Ag–Co alloy catalysts for electrochemical oxygen reduction. *Nat. Chem.* **2014,** *6*, 828.
5. Shao, M.; Chang, Q.; Dodelet, J.-P.; Chenitz, R., Recent Advances in Electrocatalysts for Oxygen Reduction Reaction. *Chem. Rev.* **2016,** *116*, 3594-3657.
6. Van Cleve, T.; Gibara, E.; Linic, S., Electrochemical Oxygen Reduction Reaction on Ag Nanoparticles of Different Shapes. *Chem. Cat. Chem.* **2015,** *8*, 256-261.
7. Zhou, R.; Zheng, Y.; Jaroniec, M.; Qiao, S.-Z., Determination of the Electron Transfer Number for the Oxygen Reduction Reaction: From Theory to Experiment. *ACS Catal.* **2016,** *6*, 4720-4728.
8. Yang, X.; Gan, L.; Zhu, C.; Lou, B.; Han, L.; Wang, J.; Wang, E., A dramatic platform for oxygen reduction reaction based on silver nanoclusters. *Chem. Comm.* **2014,** *50*, 234-236.
9. Tian, Y.; Wang, F.; Liu, Y.; Pang, F.; Zhang, X., Green synthesis of silver nanoparticles on nitrogen-doped graphene for hydrogen peroxide detection. *Electrochim. Acta* **2014,** *146*, 646-653.
10. Slanac, D. A.; Hardin, W. G.; Johnston, K. P.; Stevenson, K. J., Atomic [1] Ensemble and Electronic Effects in Ag-Rich AgPd Nanoalloy Catalysts for Oxygen Reduction in Alkaline Media. *J. Am. Chem. Soc.* **2012,** *134*, 9812-9819.
11. García-Contreras, M. A.; Fernández-Valverde, S. M.; Basurto-Sánchez, R., Investigation of oxygen reduction in alkaline media on electrocatalysts prepared by the mechanical alloying of Pt, Co, and Ni. *J. Appl. Electrochem.* **2015,** *45*, 1101-1112.
12. Higgins, D.; Wette, M.; Gibbons, B. M.; Siahrostami, S.; Hahn, C.; Escudero-Escribano, M. A.; García-Melchor, M.; Ulissi, Z.; Davis, R. C.; Mehta, A.; Clemens, B. M.; Nørskov, J. K.; Jaramillo, T. F., Copper Silver Thin Films with Metastable Miscibility for Oxygen Reduction Electrocatalysis in Alkaline Electrolytes. *ACS Appl. Energy Mater.* **2018,** *1*, 1990-1999.
13. Mukherjee, D.; P, M. A.; Sampath, S., Few-Layer Iron Selenophosphate, FePSe3: Efficient Electrocatalyst toward Water Splitting and Oxygen Reduction Reactions. *ACS Appl. Energy Mater.* **2018,** *1*, 220-231.
14. Yang, Z.; Ling, Y.; Zhang, Y.; Xu, G., High Performance Palladium Supported on Nanoporous Carbon under Anhydrous Condition. *Sci. Rep.* **2016,** *6*, 36521.
15. Zhou, R.; Qiao, S. Z., Silver/Nitrogen-Doped Graphene Interaction and Its Effect on Electrocatalytic Oxygen Reduction. *Chem. Mater.* **2014,** *26*, 5868-5873.
16. Hernández-Rodríguez, M. A.; Goya, M. C.; Arévalo, M. C.; Rodríguez, J. L.; Pastor, E., Carbon supported Ag and Ag–Co catalysts tolerant to methanol and ethanol for the oxygen reduction reaction in alkaline media. *Int. J. Hydrog. Energy* **2016,** *41*, 19789-19798.

17. Blizanac, B. B.; Ross, P. N.; Marković, N. M., Oxygen Reduction on Silver Low-Index Single-Crystal Surfaces in Alkaline Solution: Rotating Ring DiskAg(hkl) Studies. *J. Phys. Chem. B* **2006,** *110*, 4735-4741.
18. Yuan, L.; Jiang, L.; Liu, J.; Xia, Z.; Wang, S.; Sun, G., Facile synthesis of silver nanoparticles supported on three dimensional graphene oxide/carbon black composite and its application for oxygen reduction reaction. *Electrochim. Acta* **2014,** *135*, 168-174.
19. Zhang, Z.; Xu, F.; Yang, W.; Guo, M.; Wang, X.; Zhang, B.; Tang, J., A facile one-pot method to high-quality Ag-graphene composite nanosheets for efficient surface-enhanced Raman scattering. *Chem. Comm.* **2011,** *47*, 6440-6442.
20. Lee, C.-L.; Chiou, H.-P.; Chang, K.-C.; Huang, C.-H., Carbon nanotubes-supported colloidal Ag–Pd nanoparticles as electrocatalysts toward oxygen reduction reaction in alkaline electrolyte. *Int. J. Hydrog. Energy* **2011,** *36*, 2759-2764.
21. Santiago, D.; Cruz-Quiñonez, M.; Tryk, D. A.; Cabrera, C. R., Pt/C Catalyst Preparation Using Rotating Disk-Slurry Electrode (RoDSE) Technique. *ECS Trans.* **2007,** *3*, 35-40.
22. Santiago, D.; Rodríguez-Calero, G. G.; Rivera, H.; Tryk, D. A.; Scibioh, M. A.; Cabrera, C. R., Platinum Electrodeposition at High Surface Area Carbon Vulcan-XC-72R Material Using a Rotating Disk-Slurry Electrode Technique. *J. Electrochem. Soc.* **2010,** *157*, F189-F195.
23. Santiago, D.; Rodriguez-Calero, G. G.; Palkar, A.; Barraza-Jimenez, D.; Galvan, D. H.; Casillas, G.; Mayoral, A.; José-Yacamán, M.; Echegoyen, L.; Cabrera, C. R., Platinum Electrodeposition on Unsupported Carbon Nano-Onions. *Langmuir* **2012,** *28*, 17202-17210.
24. Betancourt, L. E.; Guzmán-Blas, R.; Luo, S.; Stacchiola, D. J.; Senanayake, S. D.; Guinel, M.; Cabrera, C. R., Rotating Disk Slurry Au Electrodeposition at Unsupported Carbon Vulcan XC-72 and Ce3+ Impregnation for Ethanol Oxidation in Alkaline Media. *Electrocatalysis* **2017,** *8*, 87-94.
25. Jesus, E. C.-d.; Santiago, D.; Casillas, G.; Mayoral, A.; Magen, C.; José-Yacaman, M.; Li, J.; Cabrera, C. R., Platinum Electrodeposition on Unsupported Single Wall Carbon Nanotubes and Its Application as Methane Sensing Material. *J. Electrochem. Society* **2012,** *160*, H98-H104.
26. Cunci, L.; Rao, C. V.; Velez, C.; Ishikawa, Y.; Cabrera, C. R., Graphene-Supported Pt, Ir, and Pt-Ir Nanoparticles as Electrocatalysts for the Oxidation of Ammonia. *Electrocatalysis* **2013,** *4*, 61-69.
27. Suleiman, A.; Menéndez, C. L.; Polanco, R.; Fachini, E. R.; Hernández-Lebrón, Y.; Guinel, M. J. F.; Roque-Malherbe, R.; Cabrera, C. R., Rotating disk slurry electrodeposition of platinum at Y-zeolite/carbon Vulcan XC-72R for methanol oxidation in alkaline media. *RSC Adv.* **2015,** *5*, 7637-7646.
28. Ahmed, M. S.; Lee, D.-W.; Kim, Y.-B., Graphene Supported Silver Nanocrystals Preparation for Efficient Oxygen Reduction in Alkaline Fuel Cells. *J. Electrochem. Soc.* **2016,** *163*, F1169-F1176.
29. Su, C.-Y.; Xu, Y.; Zhang, W.; Zhao, J.; Tang, X.; Tsai, C.-H.; Li, L.-J., Electrical and Spectroscopic Characterizations of Ultra-Large Reduced Graphene Oxide Monolayers. *Chem. Mater.* **2009,** *21* (23), 5674-5680.
30. Ahmed, M. S.; Jeon, S., New functionalized graphene sheets for enhanced oxygen reduction as metal-free cathode electrocatalysts. *J. Power Sources* **2012,** *218*, 168-173.
31. Hsiao, M.-C.; Liao, S.-H.; Yen, M.-Y.; Liu, P.-I.; Pu, N.-W.; Wang, C.-A.; Ma, C.-C. M., Preparation of Covalently Functionalized Graphene Using Residual Oxygen-Containing Functional Groups. *ACS Appl. Mater. Interfaces* **2010,** *2* (11), 3092-3099.

32. Ahmed, M. S.; Han, H. S.; Jeon, S., One-step chemical reduction of graphene oxide with oligothiophene for improved electrocatalytic oxygen reduction reactions. *Carbon* **2013,** *61*, 164-172.
33. Ahmed, M. S.; Jeon, S., Electrochemical activity evaluation of chemically damaged carbon nanotube with palladium nanoparticles for ethanol oxidation. *J. Power Sources* **2015,** *282*, 479-488.
34. Socrates, G., *IInfrared and Raman Characteristic Group Frequencies: Tables and Charts, 3rd Edition*. John Wiley and Sons: 2004.
35. Chen, W.; Yan, L.; Bangal, P. R., Chemical Reduction of Graphene Oxide to Graphene by Sulfur-Containing Compounds. *J. Phys. Chem. C* **2010,** *114*, 19885-19890.
36. Pérez-Rodríguez, S.; Pastor, E.; Lázaro, M. J., Electrochemical behavior of the carbon black Vulcan XC-72R: Influence of the surface chemistry. *Int. J. Hydrog. Energy* **2018,** *43*, 7911-7922.
37. Lázaro, M. J.; Calvillo, L.; Celorrio, V.; Pardo, J.; Perathoner, S.; Moliner, R., Study and application of Vulcan XC-72 in low temperature fuel cells. In *Carbon Black: Production, Properties and Uses*, Nova Science Publisher, Inc, New York: 2011; pp 41-68.
38. Vi, T. T. T.; Rajesh Kumar, S.; Rout, B.; Liu, C.-H.; Wong, C.-B.; Chang, C.-W.; Chen, C.-H.; Chen, D. W.; Lue, S. J., The Preparation of Graphene Oxide-Silver Nanocomposites: the Effect of Silver Loads on Gram-Positive and Gram-Negative Antibacterial Activities. *Nanomaterials (Basel)* **2018,** *8*, 163.
39. Pappas, R. S., Sample Preparation Problem Solving for Inductively Coupled Plasma-Mass Spectrometry with Liquid Introduction Systems I. Solubility, Chelation, and Memory Effects. *Spectroscopy (Springfield, Or.)* **2012,** *27*, 20-31.
40. Habekost, A., Experimental Investigations of Alkaline Silver-zinc and Copper-zinc Batteries. *World J. Chem. Educ.* **2016,** *4*, 4-12.
41. Joo, Y.; Ahmed, M.; Soon Han, H.; Jeon, S., Preparation Of Electrochemically Reduced Graphene Oxide-Based Silver-Cobalt Alloy Nanocatalysts for Efficient Oxygen Reduction Reaction. 2017.